ANALOG DEVICES

AN-106
APPLICATION NOTE

ONE TECHNOLOGY WAY • P.O. BOX 9106 • NORWOOD, MASSACHUSETTS 02062-9106 • 617/329-4700

A Collection of Amp Applications

by James Wong

This note examines some of the numerous and widely-used applications of the operational amplifier. While not attempting to list every possible application, it presents several basic circuit configurations that can be modified to suit applications other than those listed. In each case, significant op amp or circuit characteristics are discussed to aid the user in adapting the circuit to a particular need. Table 1 provides an index to the applications contained in this note.

TABLE 1: Op Amp Circuit Applications

FIGURE 1: ±200mA Servo Motor Amplifier

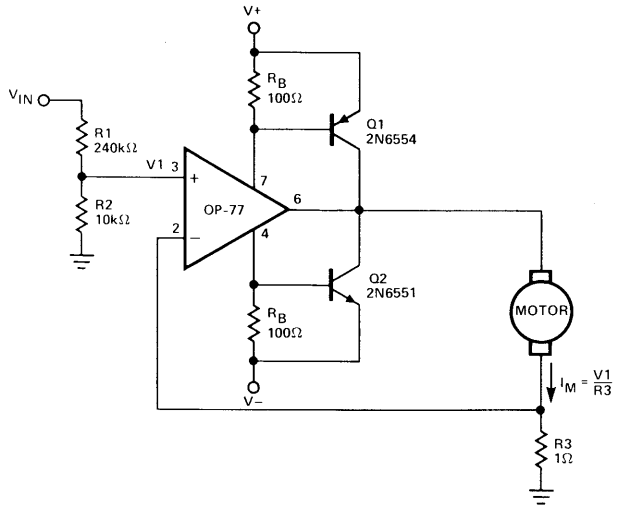

R_B sets the bias point for transistors Q1 and Q2. Because $V_{BE(ON)}$ varies greatly with temperature, a guardband is required to prevent Q1 and Q2 from conducting simultaneously. R_B should be selected such that the transistors do not conduct until I_M equals the op amp quiescent supply current, I_{SY}. The transistors will begin to conduct at about $V_{BE\,(ON)} = 0.5V$.

In this design,

$$R_B = \frac{V_{BE(ON)}}{I_{SY} + I_M} = \frac{0.5}{0.0025 + 0.0025} = 100\Omega$$

To maximize voltage swing across the motor, V1 must be minimized. If at full load V1 = 0.2V with V+ = 15V and V_{BE1} = 0.8V, the voltage across the motor will be:

$$V_M = (V^+ - 2) - V_{BE1} - V1 = (15 - 2) - 0.8 - 0.2$$
$$= 12.0V$$

V_{IN} may be scaled with a resistive divider as:

$$\frac{V_{IN}}{V1} = \frac{R1 + R2}{R2}$$

With R1 = 240kΩ and R2 = 10kΩ, V_{IN} = 5V will produce I_M = 200mA.

FIGURE 2: Precision Programmable Gain Amplifier

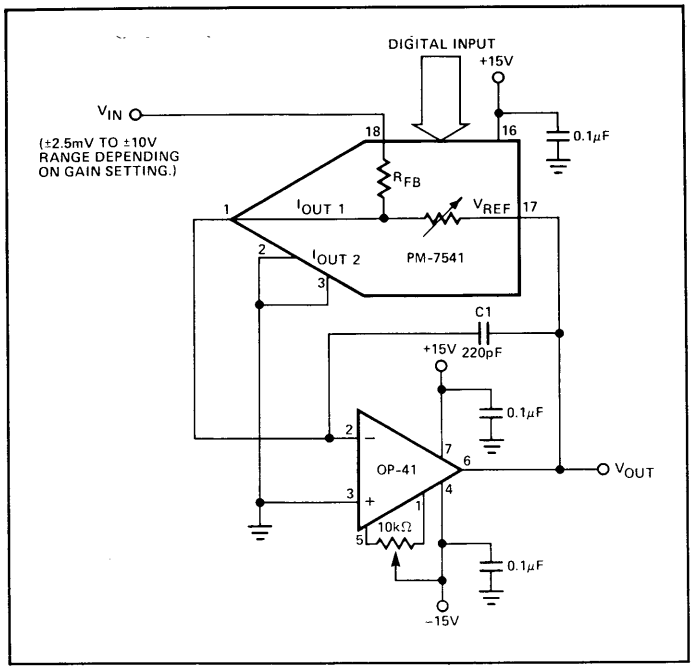

The digitally programmable gain has 12-bit accuracy over the range of −1 to −1024 and 10-bit accuracy to −4096. The low bias current of the OP-41's JFET input maintains this accuracy, while C1 limits the noise voltage bandwidth allowing accurate measurement down to microvolt levels.

DIGITAL IN	GAIN (A_V)
4095	−1.00024
2048	−2
1024	−4
512	−8
256	−16
128	−32
64	−64
32	−128
16	−256
8	−512
4	−1024
2	−2048
1	−4096
0	OPEN LOOP

FIGURE 3: Bilateral Current Source

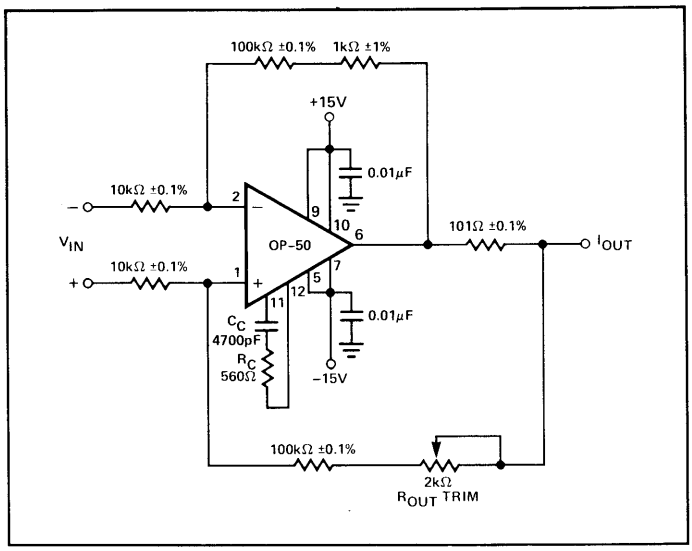

Compliance is better than ±11V at an output current of 20mA, and the trimmed output resistance is typically 2MΩ with $R_L \leq 500\Omega$. For the resistor values shown, the maximum V_{IN} is 200mV.

FIGURE 4: Precision Current Pump

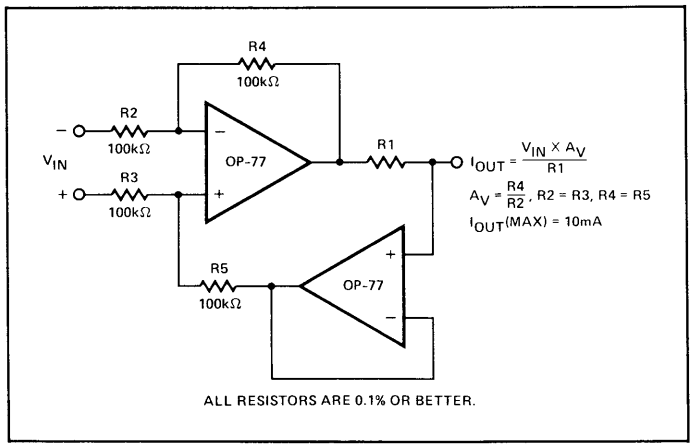

Accuracy of I_{OUT} is improved by using a noninverting voltage-follower in the feedback loop. To maximize voltage compliance of I_{OUT}, R1 should be minimized.

FIGURE 5: High-Sensitivity Voltage Comparator

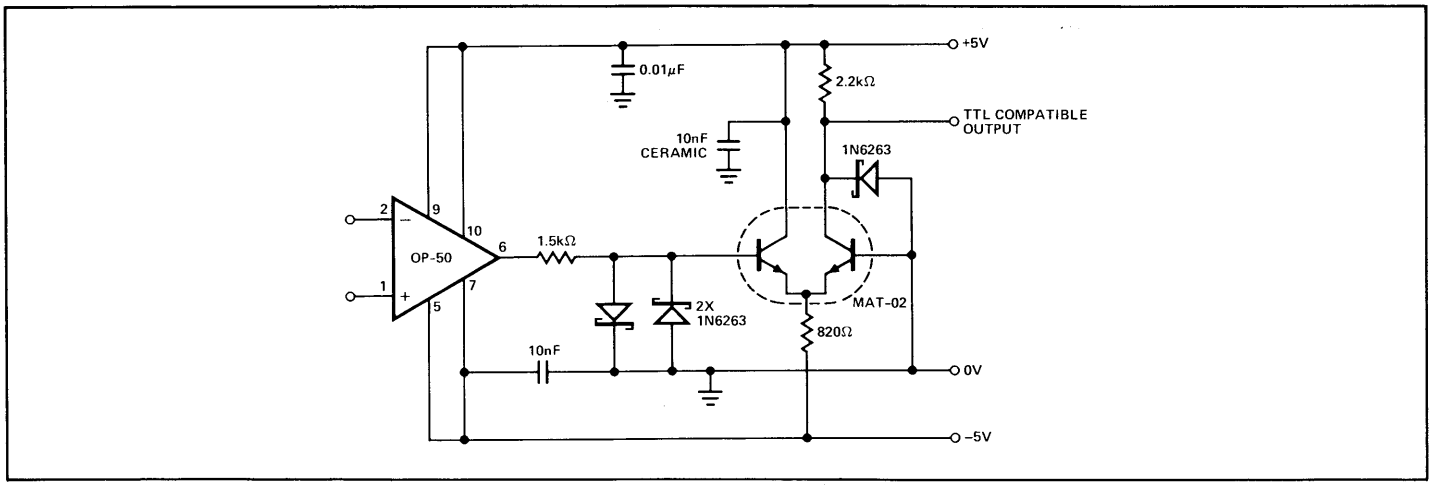

This comparator circuit is capable of resolving a submicrovolt difference signal. The OP-50, operating without feedback, drives a second gain stage which generates a TTL-compatible output signal. Schottky-clamp diodes prevent overdriving of the long-tailed transistor pair and stop saturation of the output transistor. Power supply voltage is set to ±5V to lower the quiescent power dissipation and minimize thermal feedback due to output stage dissipation. Operating from ±5V supplies also reduces the OP-50 rise and fall times as the output slews over a reduced voltage range. This, in turn, reduces the output response time.

It is common practice with voltage comparators to ground one input terminal and to use a single-ended input. The historic reason is poor common-mode rejection on the input stage. In contrast, the OP-50 has very high common-mode rejection and is capable of detecting microvolt level differences in the presence of large common-mode signals.

The comparator is not fast, but it is very sensitive and can detect signal differences as low as 0.3μV. With large input overdrives, the circuit responds in approximately 3μs. If sharp transitions are needed, the use of a TTL Schmitt-trigger input is recommended. A table of Response Time vs. Input Overdrive is shown below.

INPUT OVERDRIVE	100mV	10mV	1mV	100μV	10μV
Positive Output Delay	3.2μs	5μs	40μs	340μs	2.4ms
Negative Output Delay	1.8μs	5μs	50μs	380μs	4.5ms

FIGURE 6: Micropower 5V Regulator

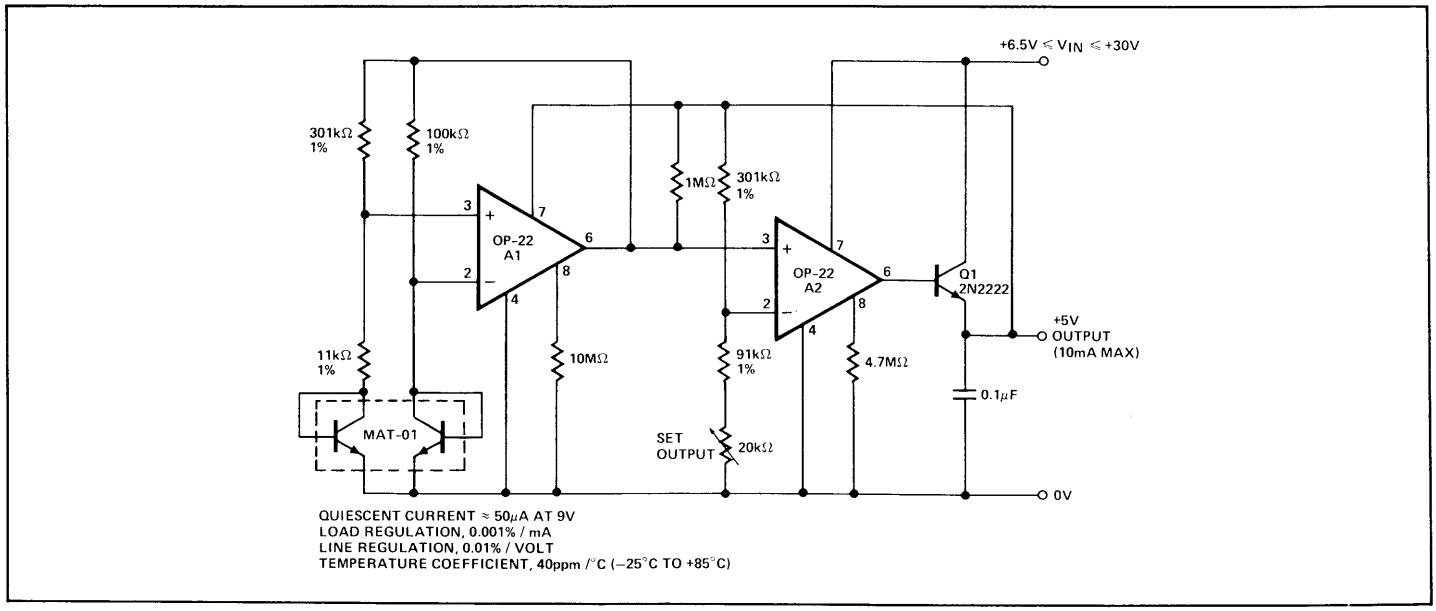

This 5V regulator is ideal for instrumentation requiring good power efficiency. Low-power 3-terminal IC regulators typically draw 2mA to 5mA quiescent current compared to only 50μA with this discrete implementation. Maximum load current is 10mA as shown, and can be increased by changing Q1 to a power transistor and proportionately increasing the set current of A2.

FIGURE 7: Micropower 1.23V Bandgap Reference

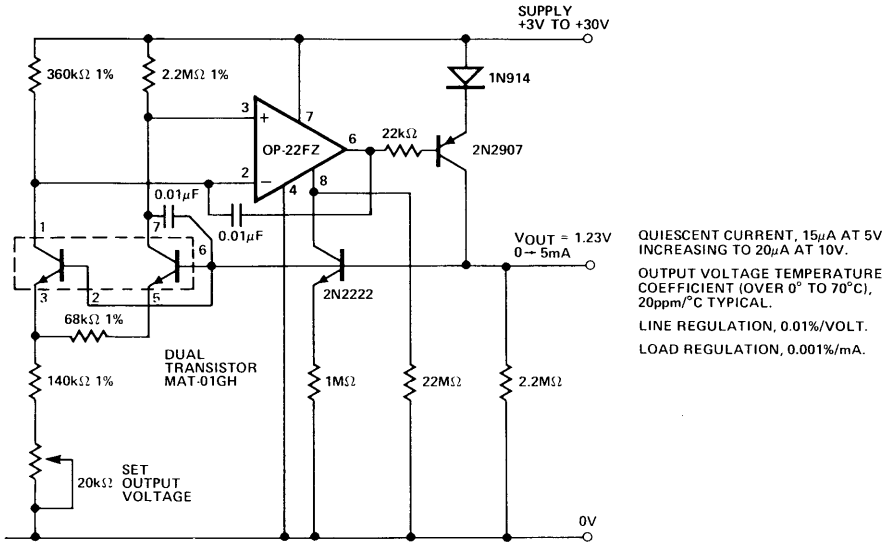

A micropower bandgap voltage reference operating at a quiescent current of 15μA may be constructed using an OP-22 and a MAT-01 dual transistor. The circuit provides a 1.23V reference with better performance than micropower IC shunt regulators and has the advantages of being a series regulator.

FIGURE 8: Versatile Triangular Wave Generator

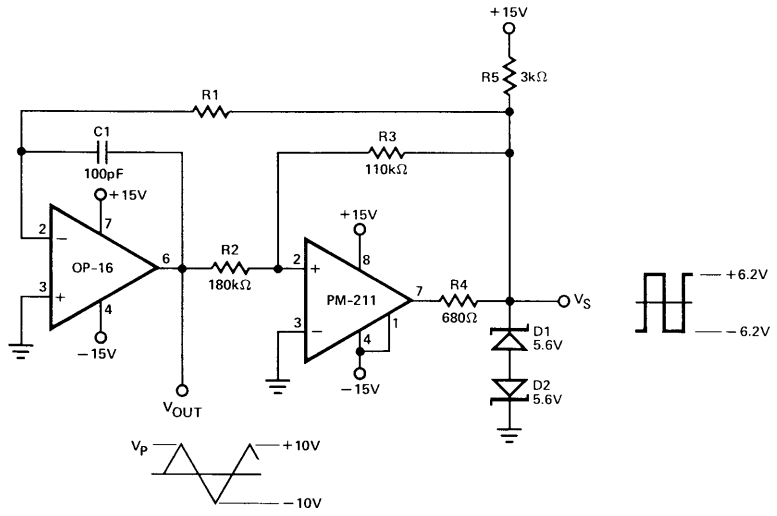

Triangular waveshapes of ±10V from 100Hz to 500kHz are obtained with values of R1 from 15MΩ to 3kΩ as given by:

$$R1 = \frac{V_S}{4V_P \cdot f_O \cdot C1}, \; V_S = 6.2V, \; V_P = 10V$$

The amplitude of the triangle wave may be adjusted via R2 as:

$$R2 = \frac{V_P \cdot 110k\Omega}{6.2V}$$

FIGURE 9: Wide Range, Low Current Ammeter

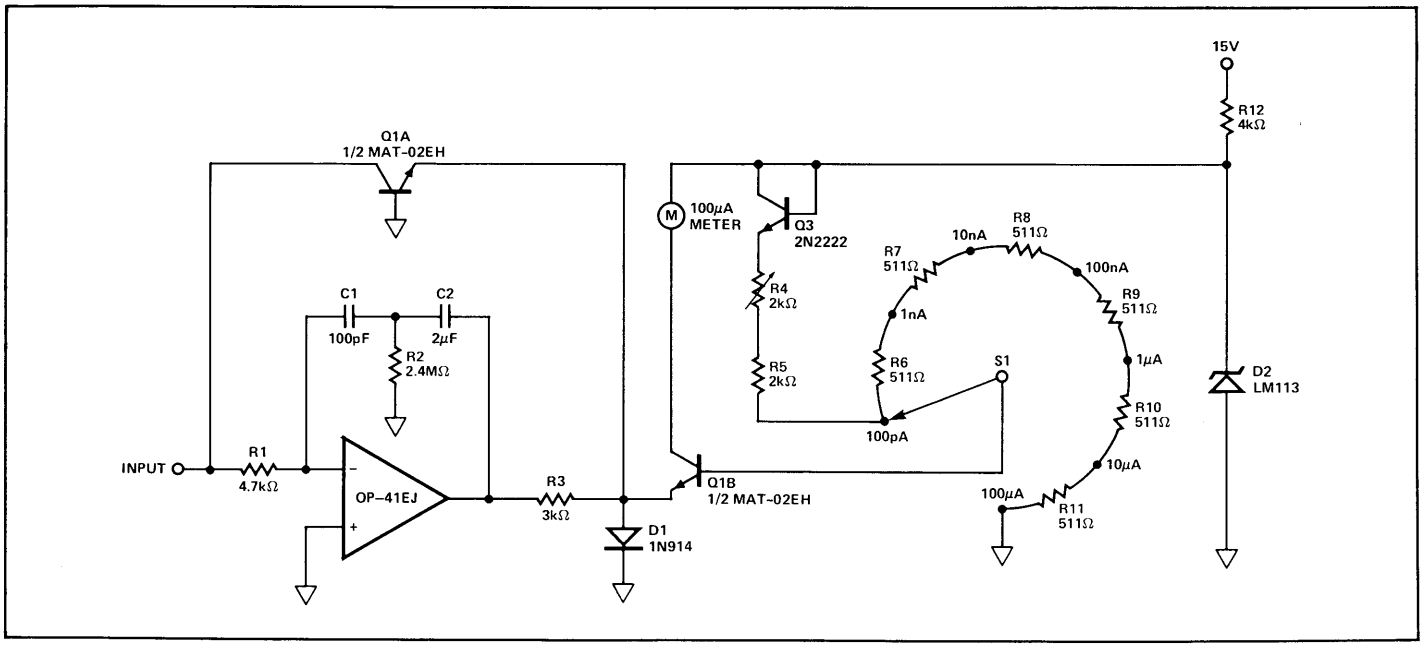

This ammeter can measure currents from 100pA to 100μA without the use of high value resistors. Accuracy is better than 1% over most of the range, depending upon the accuracy of the divider resistor and the input bias current of the op amp. Using the OP-41 as the input amplifier allows low end measurement down to a few pA due to the 5pA input bias current. Because the voltage across the inputs of the inverting amplifier is forced to virtually zero, the current meter's effective series voltage drop is less than 500μV at any current level.

Calibration is simple, requiring only one adjustment. R4 is used to adjust full scale deflection with a 1μA input current. This will give maximum accuracy over the operating range of currents.

The low V_{OS} and exceptionally good log conformance of the MAT-02 assure high accuracy over the full 6 decade operating range.

FIGURE 10: Precision Threshold Detector/Amplifier

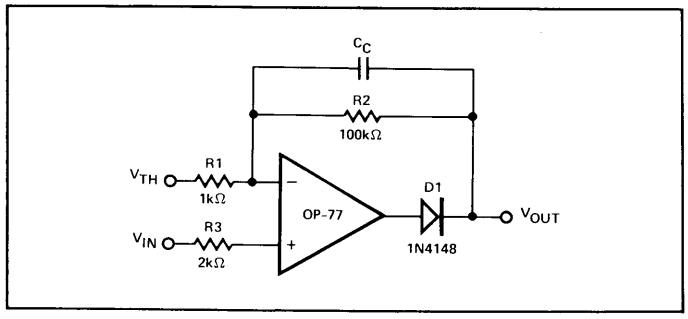

When $V_{IN} < V_{TH}$, the amplifier output swings negative, reverse biasing diode D1. Therefore $V_{OUT} = V_{TH}$.

When $V_{IN} \geq V_{TH}$, the loop closes, and

$$V_{OUT} = V_{TH} + (V_{IN} - V_{TH})\left(1 + \frac{R2}{R1}\right)$$

C_C is selected to smooth the loop response.

FIGURE 11: Wide-Dynamic-Range Light Detector

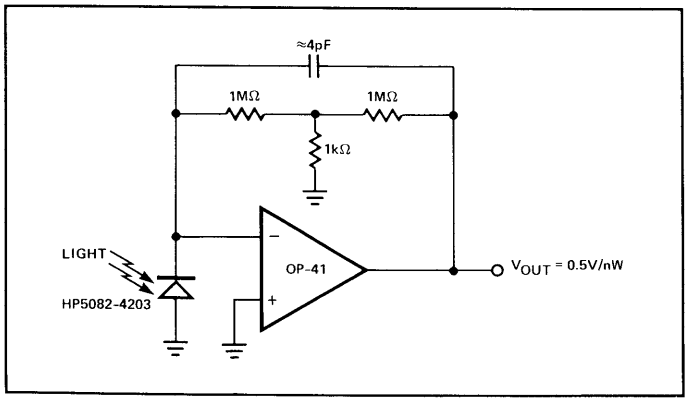

This circuit produces an output voltage proportional to light input over a 60dB range. The 5pA input bias current of the OP-41 assures a low output voltage offset.

FIGURE 12: Isolation Amplifier

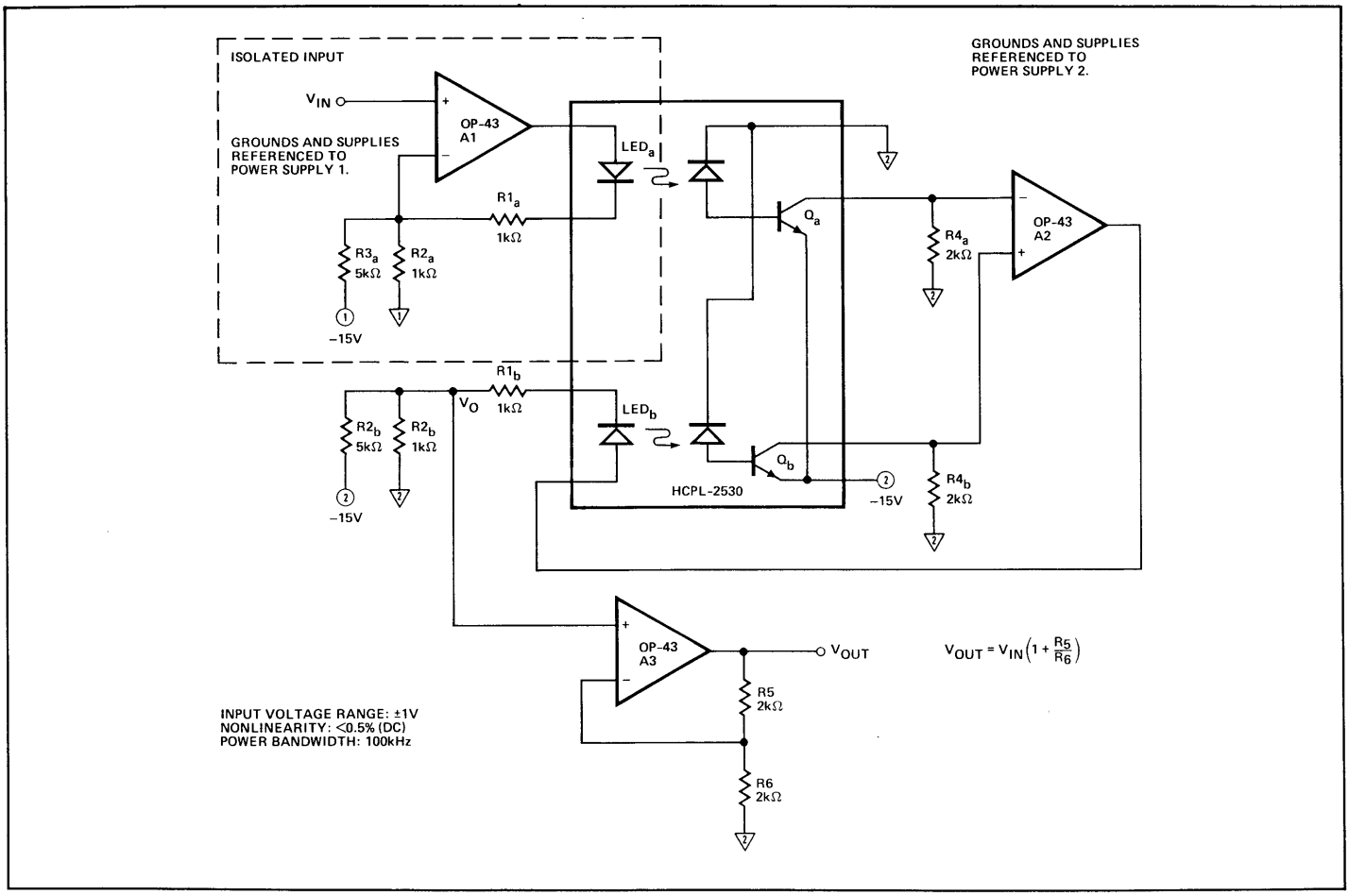

In conjunction with two optocouplers, or a dual optocoupler such as the Hewlett-Packard HCPL-2530, three OP-43's can be combined to create an isolation amplifier. In this sort of amplifier, the input and the output operate on separate power supplies, allowing extremely high common-mode voltages to be dealt with. In industrial applications, an isolation amplifier protects instrumentation from high voltages at the sensing site. When interfacing with a computing system, an isolation amplifier will protect the rest of the system from a sensor which accidentally becomes shorted to a high voltage.

The isolation amplifier operates on the principle that the nonlinearities of one optocoupler will be tracked by the nonlinearities of another, if they are well matched. By using an optocoupler in the feedback loop of A2, nonlinearities of the isolating optocoupler will be cancelled. V_O will equal V_{IN} plus an offset created by imperfect matching between a and b side resistors and optocouplers.

A3 is an output buffer for the isolation amplifier. The low bias current ensures that it does not affect the voltage it is amplifying. Gain is realized in this stage, and any offsets induced in the previous stages may be corrected by offsetting this op amp. Although shown in the circuit as a simple gain stage, this output amplifier may take any form desired. It may be configured as a filter or other waveshaping circuit as needed. The only requirement is that the buffer not disturb the currents in the optocoupler feedback circuit, thus noninverting amplifier configurations are preferred. For highest linearity, the currents in the two LEDs should track as closely as possible.

With stable supplies, the circuit has excellent reponse and displays less than 0.5% DC nonlinearity with a $2V_{p-p}$ signal. The high speed of the OP-43 gives the circuit a power bandwidth of 100kHz, while the majority of the power budget is consumed in biasing the LEDs. The dual optocoupler provides isolation against 600VDC common-mode voltages. Higher isolations may be achieved using two separate optocouplers, such as HP's 6N136.

FIGURE 13: Dual Programmable Window Comparator

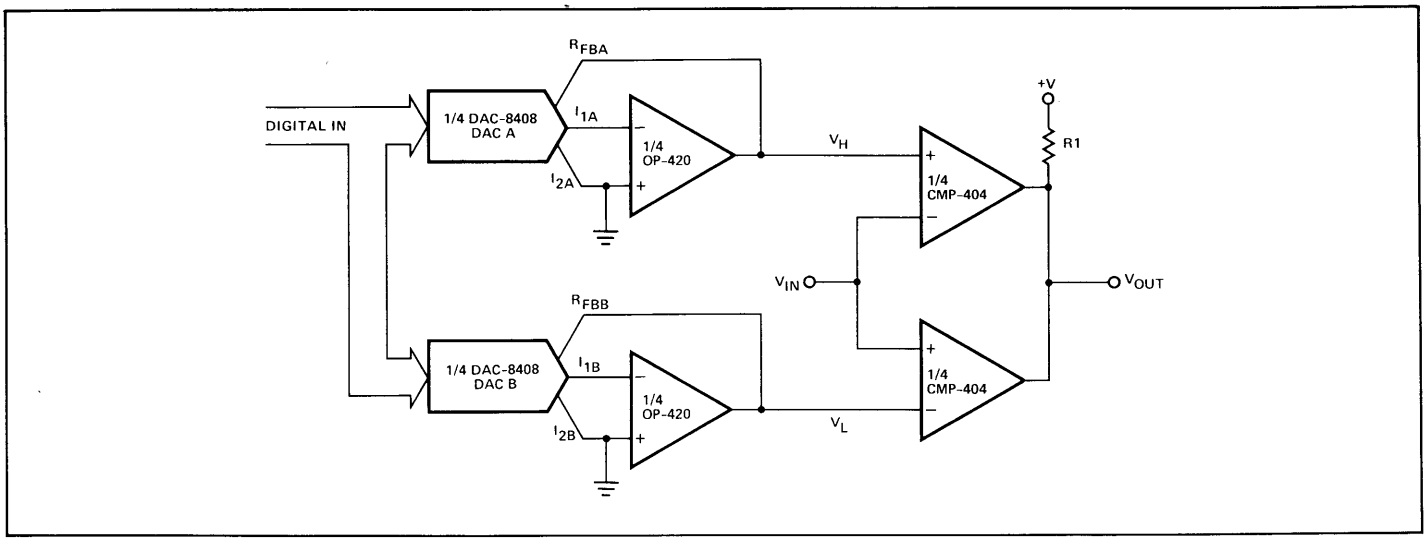

Only three ICs are required to fully implement two independent programmable window comparators. The quad, latched, 8-bit CMOS DAC-8408 together with the quad micropower OP-420 provide digitally-programmable HIGH and LOW thresholds to the CMP-404, quad low-power comparator. The outputs of the threshold comparators are wire-ORed with a common pull-up resistor producing $V_{OUT} = +V$ only when $V_L < V_{IN} < V_H$. Total supply current for the full circuit is less than 2mA.

FIGURE 14: ±36V Low Noise Operational Amplifier

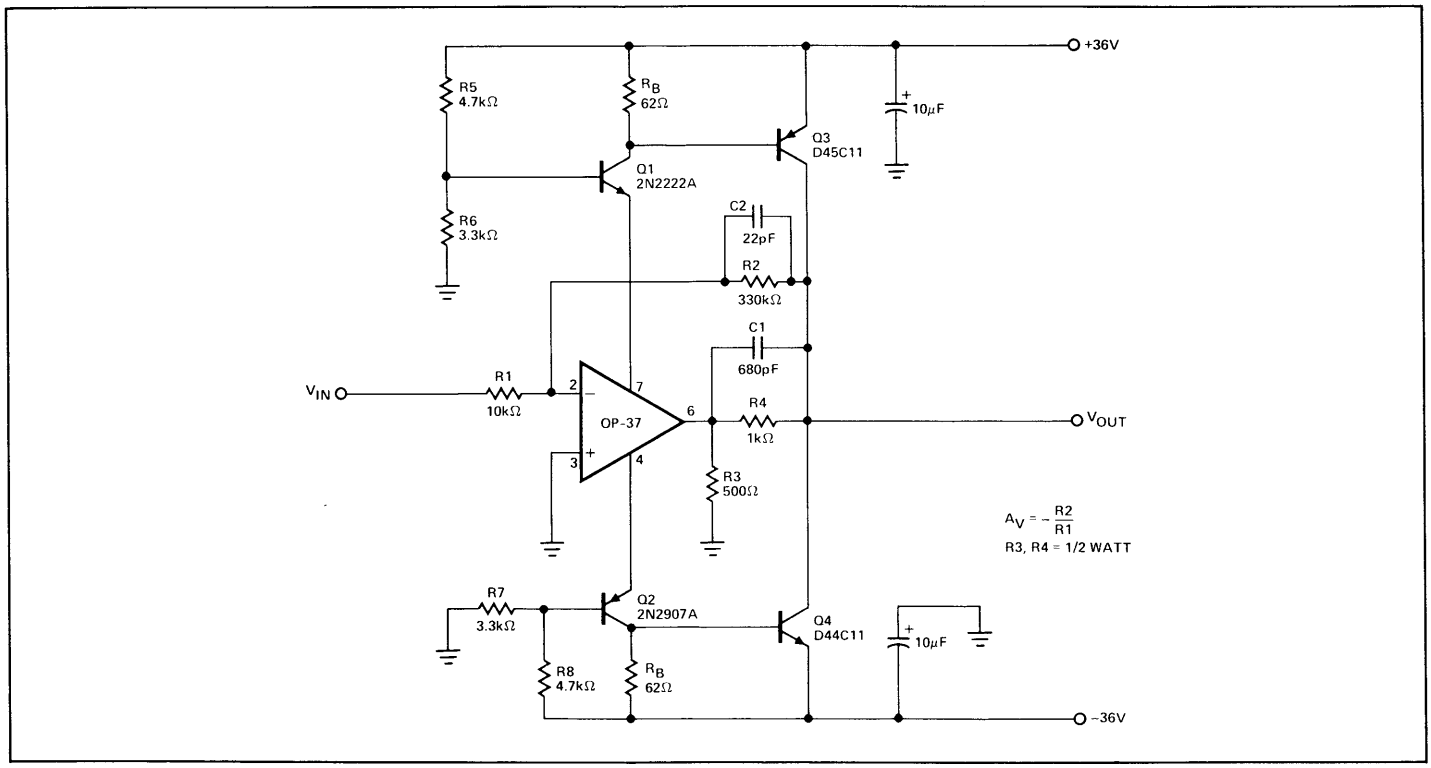

An OP-37 provides a low-noise front end for this amplifier which is capable of delivering over ±200mA to a load with a 70V peak-to-peak output swing. Transistors Q1 and Q2 are series regulators stepping down the supply voltage for the OP-37 to ±15V, while transistors Q3 and Q4 provide the high current output drive. R3 and R4 form an output voltage gain stage whose gain, $A_V = 3$, is reduced to unity at high frequencies by C1 to maintain stability.

FIGURE 15: High Q Notch Filter

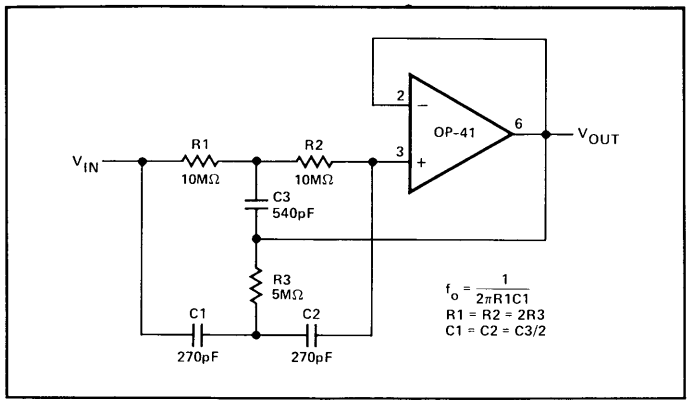

The low bias current and high input impedance of the OP-41 enable small value capacitors and large resistors to be used in this 60Hz notch filter. The 5pA bias current only develops 100μV across R1 and R2.

FIGURE 16: Piezoelectric Transducer Amplifier

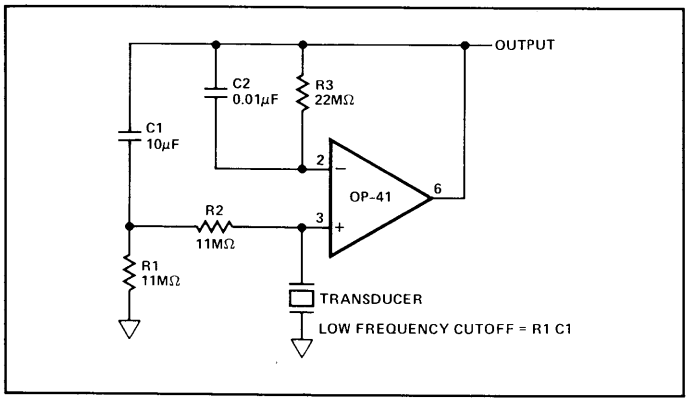

Piezoelectric transducers often require a high-input-resistance amplifier. The OP-41 can provide input resistance in the range of $10^{12}\Omega$, however, a DC return for bias current is needed. To maintain a high R_{IN}, large value resistors above 22MΩ are often required. These may not be practicable.

Using this circuit, input resistances that are orders of magnitude greater than the values of the DC return resistors can be obtained. This is accomplished by bootstrapping the resistors to the output. With this arrangement, the lower cutoff frequency is determined more by the RC product of R1 and C1 that it is by resistor values and the equivalent capacitance of the transducer.

FIGURE 17: High Stability Voltage Reference

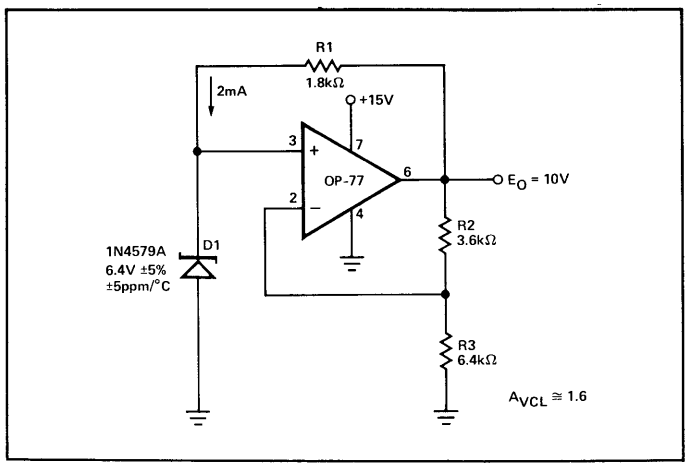

The simple bootstrapped voltage reference provides a precise 10V virtually independent of changes in power supply voltage, ambient temperature, and output loading. Correct zener operating current of exactly 2mA is maintained by R1, a selected 5ppm/°C resistor, connected to the regulated output. Accuracy is primarily determined by three factors: the 5ppm/°C temperature coefficient of D1, 1ppm/°C ratio tracking of R2 and R3, and operational amplifier V_{OS} errors. The OP-77, with TCV_{OS} of 0.3μV/°C, contributes only 0.05ppm/°C of output error, thus effectively eliminating TCV_{OS} as an error consideration.

FIGURE 18. Precision Dual Tracking Voltage References

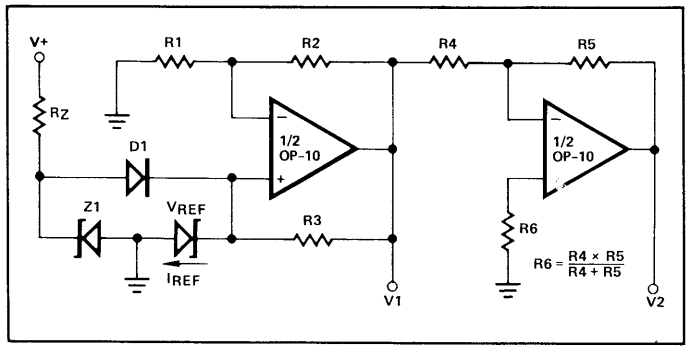

Precision dual tracking voltage references using a single reference source are easily constructed using OP-10. These references exhibit excellent stability vs. temperature/time, low noise, and excellent power supply rejection.

In the circuit shown, R3 should be adjusted to set I_{REF} to operate V_{REF} at its minimum temperature coefficient current. Proper circuit start-up is assured by R_Z, Z1, and D1.

$$V_{Z1} \leq V_{REF} \qquad V1 = V_{REF}\left(1 + \frac{R2}{R1}\right)$$

$$R3 = \frac{(V1 - V_{REF})}{I_{REF}} \qquad V2 = V1\left(\frac{-R5}{R4}\right)$$

Output Impedance (ΔI_L:1.0mA—5.0mA) ..... $0.25 \times 10^{-3}\Omega$

FIGURE 19: RIAA Phone Pre-Amplifier

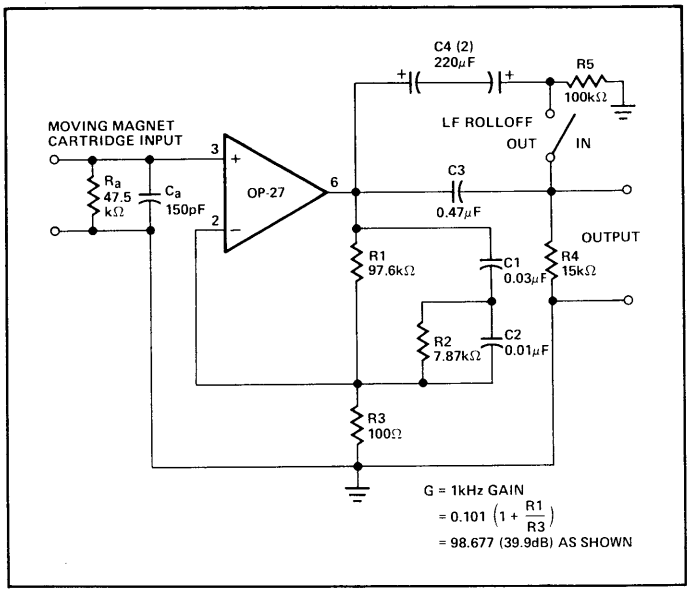

The OP-27 is used in this phono pre-amplifier circuit because of its low noise characteristics. It contributes only 3.2nV/$\sqrt{\text{Hz}}$ voltage noise and 0.45pA/$\sqrt{\text{Hz}}$ current noise to the circuit. To minimize noise from other sources, R3 is set to 100Ω. This generates additional voltage noise of only 1.3nV/$\sqrt{\text{Hz}}$. With a 1kΩ source, the circuit noise measures 63dB below a 1mV reference level, unweighted, in a 20kHz bandwidth.

R1, R2, C1, and C2 form a very accurate RIAA network with standard component values providing the necessary time constants of 3180, 318, and 75µsec. For initial equalization accuracy and stability, precision metal-film resistors and film capacitors of polystyrene or polypropylene are recommended since they have low voltage coefficients, dissipation factors, and dielectric absorption. (High-K ceramic capacitors should be avoided here, though low-K ceramics—such as NPO types, which have excellent dissipation factors, and somewhat lower dielectric absorption—can be considered for small values.)

Capacitor C3 and resistor R4 form a simple −6dB-per-octave rumble filter, with a corner at 22Hz. As an option, the switch-selected shunt capacitor C4, a nonpolarized electrolytic, bypasses the low-frequency rolloff. Placing the rumble filter's high-pass action after the pre-amp has the desirable result of discriminating against the RIAA-amplified low-frequency noise components and pickup-produced low-frequency disturbances.

This circuit is capable of very low distortion over its entire range, generally below 0.01% at levels up to 7Vrms. At 3V output levels, it will produce less than 0.03% total harmonic distortion at frequencies up to 20kHz.

FIGURE 20: Headphone Amplifier

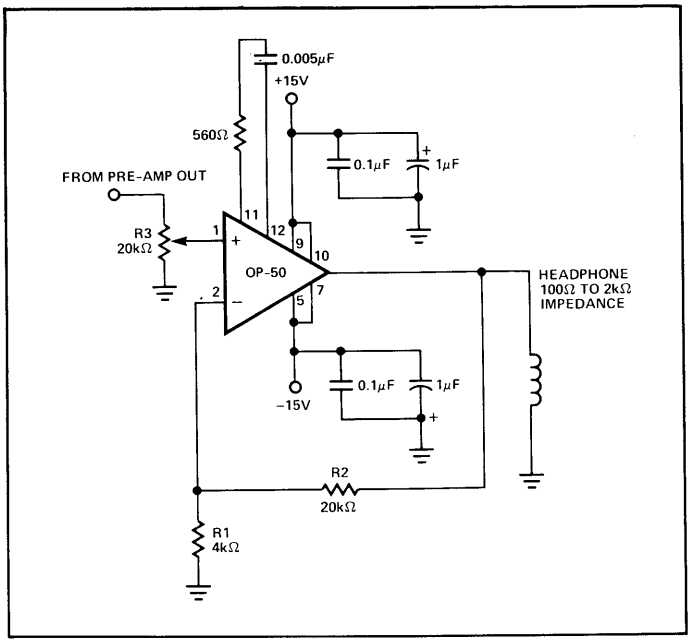

For low level Pre-Amp Out signals, the amplifier gain may be increased by reducing R1 according to:

$$R1 = \frac{20k\Omega}{A_V - 1}$$

Note that two amplifiers are required for stereo applications.

Performance: (V_{OUT} = 6V_{RMS}, R1 = 4kΩ)

T.H.D @ 100Hz = 0.0025%

@ 1kHz = 0.003%

@ 10kHz = 0.011%

Signal-to-Noise Ratio ≥ 80dB

Response Flatness = ±0.4dB from 10Hz to 20kHz

Bandwidth = −3dB @ 56kHz

FIGURE 21: NAB Tape Head Pre-Amplifier

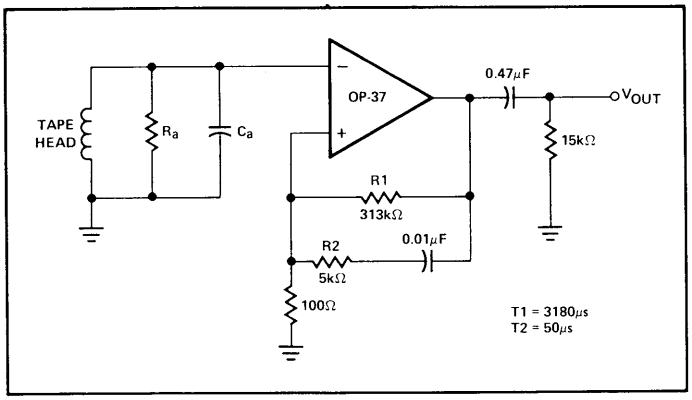

A pre-amplifier for NAB tape playback is similar to an RIAA phono pre-amp, though more gain is typically demanded, along with equalization requiring a heavy low-frequency boost.

The network values of this configuration yield a 50dB gain at 1kHz, and a DC gain greater than 70dB. Thus, the worst-case output offset is just over 500mV. The DC resistance of the tape head will add to this a bias-current-induced offset voltage. To minimize this contribution, the head's DC resistance should be low, preferably below 1kΩ. A single 0.47μF output capacitor can block the final output offset without affecting the dynamic range.

The tape head can be coupled directly to the amplifier input, since the worst-case bias current of 80nA with a 400mH, 100μin. head (such as the PRB2H7K) will not be troublesome.

One potential tape head problem is presented by amplifier bias current transients at power-up or power-down which can magnetize a head. Although the OP-37 is free of these bias current transients, it is always good design practice to control the speed of power supply rise and fall to eliminate transients.

FIGURE 22: Microphone Pre-Amplifier

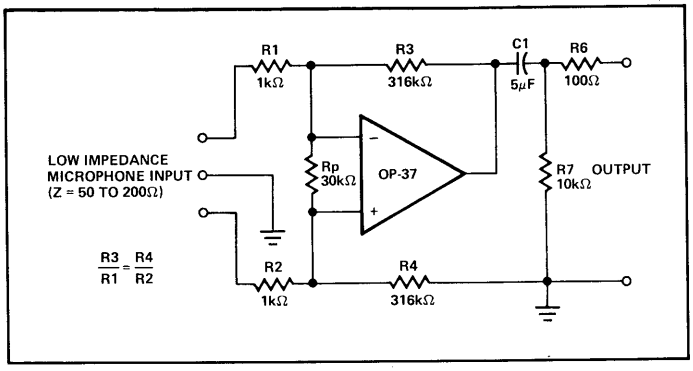

This simple, but effective, fixed-gain transformerless microphone pre-amp amplifies differential signals from low-impedance microphones by 50dB, and has an input impedance of 2kΩ. Because of the high working gain of the circuit, an OP-37 helps to preserve bandwidth, which will be 110kHz. As the OP-37 is a decompensated device (minimum stable gain of 5), a dummy resistor, R_p, may be necessary, if the microphone is to be unplugged. Otherwise the 100% feedback from the open input may cause the amplifier to oscillate.

Common-mode input-noise rejection will depend upon the match of the bridge-resistor ratios. Either close-tolerance (0.1%) types should be used, or R4 should be trimmed for best CMRR. All resistors should be metal-film types for best stability and low noise.

Noise performance of this circuit is limited more by the input resistors R1 and R2 than by the op amp, as R1 and R2 each generate a $4nV/\sqrt{Hz}$ noise, while the op amp generates a $3.2nV/\sqrt{Hz}$ noise. The rms sum of these predominant noise sources will be about $6nV/\sqrt{Hz}$, equivalent to 0.9μV in a 20kHz noise bandwidth, or nearly 61dB below a 1mV input signal. Measurements confirm this predicted performance.

FIGURE 23: Micropower Wien-Bridge Oscillator ($P_d < 500\mu W$)

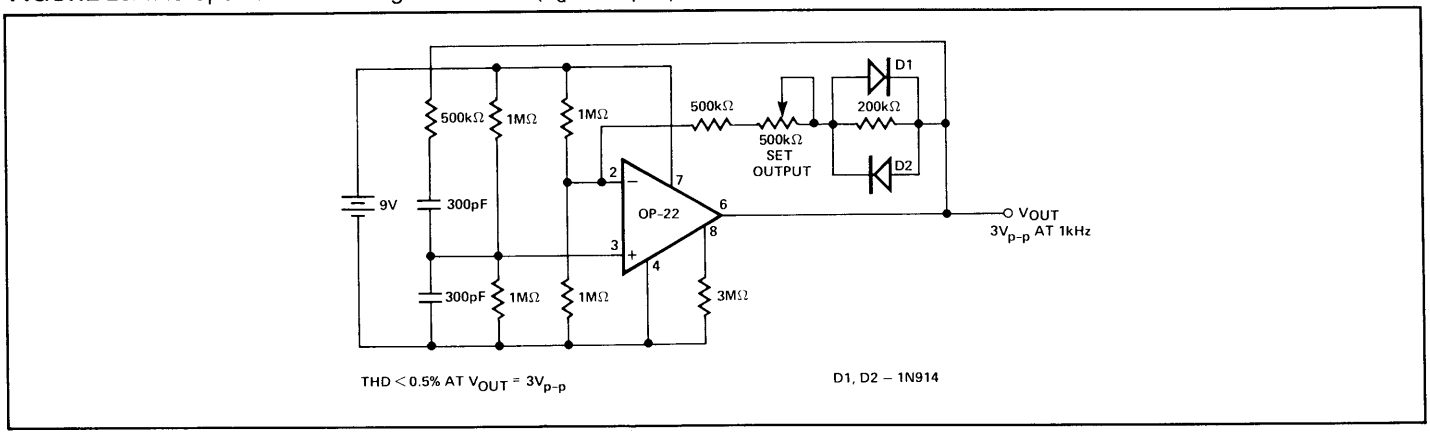

Requiring less than 60μA of supply current, this micropower Wien-bridge oscillator is ideal for battery-powered instrumentation. Output level is controlled by nonlinear elements D1 and D2. When adjusted for $3V_{p-p}$ output, the distortion level is below 0.5% at 1kHz.

FIGURE 24: Micropower Instrumentation Amplifier

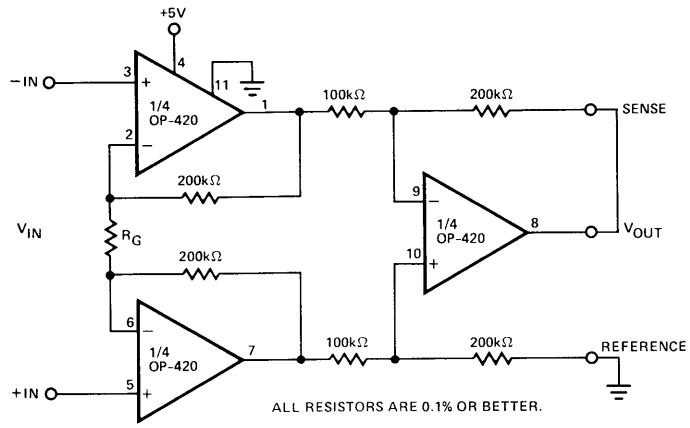

This instrumentation amplifier requires only 200μA total quiescent current (V_{CM} = 0V) and operates on single voltage supplies from +1.6V to +36V. Input and output voltage range is 0V to (V^+ − 1.5) volts with CMRR above 100dB. Differential gain, A_V, is adjusted with a single resistor, R_G, as given by:

$$R_G = \frac{800k\Omega}{A_V - 2}$$

FIGURE 25: Piecewise-Linear Amplifier (Decreasing Gain)

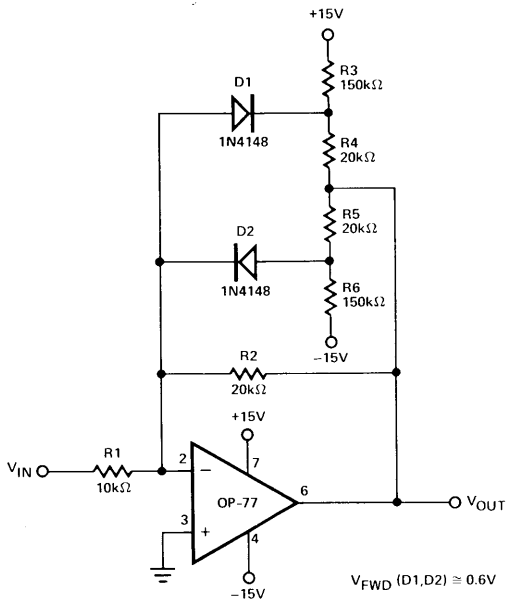

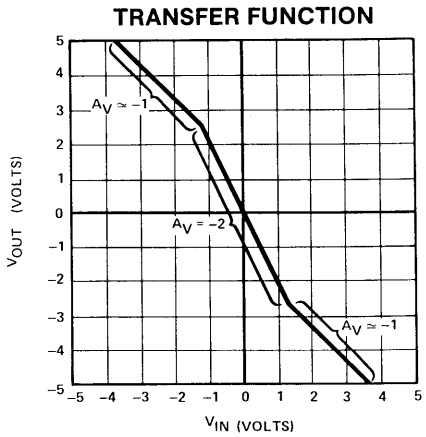

This circuit is useful in linearizing a nonlinear input signal or creating a nonlinear output function from a linear input. At V_{OUT} = 0V, both D1 and D2 are reverse biased, and V_{OUT}/V_{IN} = −R2/R1. As V_{IN} goes positive, V_{OUT} becomes negative according to that gain until a threshold is reached, $-(V_{OUT} + V_{FWD})/R4$ = 15V/R3, where D1 becomes forward biased. For more positive values of V_{IN}, the gain is:

$$\frac{V_{OUT}}{V_{IN}} = -\frac{(R2 \cdot R4)}{(R2 + R4)R1} - \frac{R2 \cdot V_{FWD}}{(R2 + R5)V_{IN}}$$

A similar action occurs as V_{IN} goes negative. Beyond the point where D2 becomes forward biased, $(V_{OUT} - V_{FWD})/R5$ = 15V/R6, the gain is:

$$\frac{V_{OUT}}{V_{IN}} = -\frac{(R2 \cdot R5)}{(R2 + R5)R1} - \frac{R2 \cdot V_{FWD}}{(R2 + R5)V_{IN}}$$

Additional diode/resistor combinations can be added to further contour the gain.

FIGURE 26: Piecewise-Linear Amplifier (Increasing Gain)

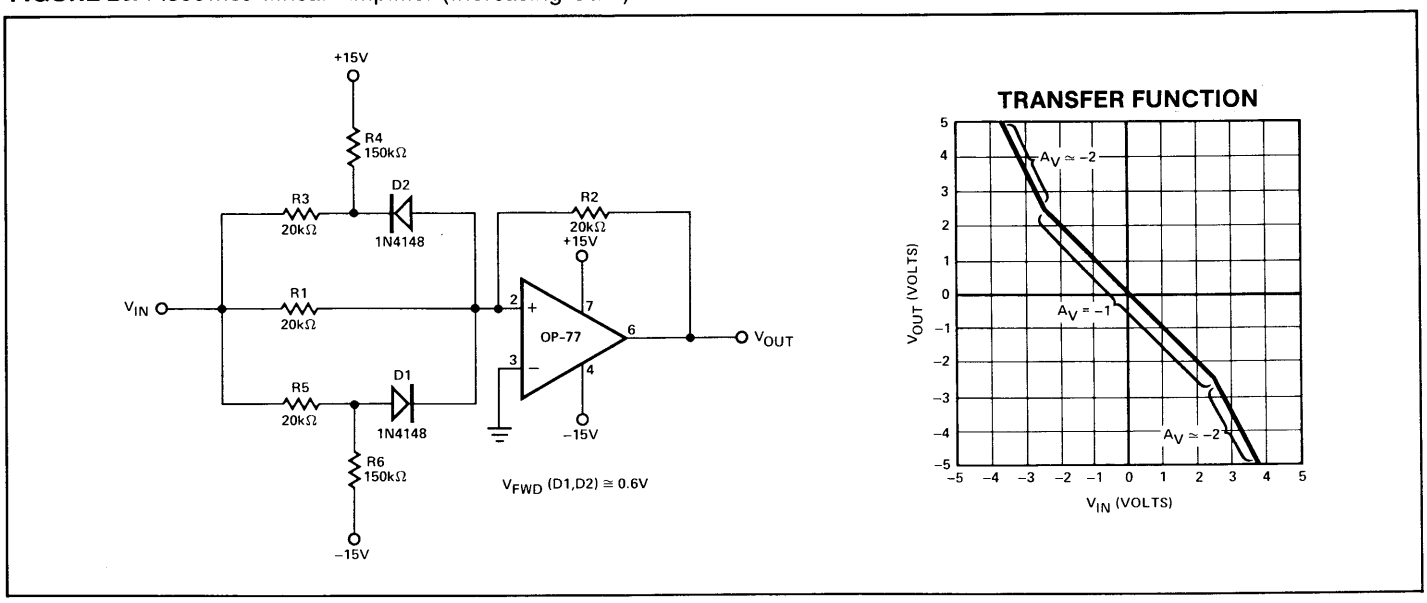

This circuit performs the linear-to-nonlinear or nonlinear-to-linear transformation by increasing gain beyond fixed thresholds. At $V_{IN} = 0V$, both D1 and D2 are reverse biased, and $V_{OUT}/V_{IN} = -R2/R1$. As V_{IN} goes positive beyond the threshold, $(V_{IN} - V_{FWD})/R5 = 15V/R6$, D1 conducts, and the gain becomes:

$$\frac{V_{OUT}}{V_{IN}} = -\frac{R2(R1 + R5)}{(R1 \cdot R5)} + \frac{V_{FWD} \cdot R2}{V_{IN} \cdot R5}$$

As V_{IN} goes negative beyond the threshold, $-(V_{IN} + V_{FWD})/R3 = 15V/R4$, D2 conducts, and the gain becomes:

$$\frac{V_{OUT}}{V_{IN}} = -\frac{R2(R1 + R3)}{(R1 \cdot R3)} + \frac{V_{FWD} \cdot R2}{V_{IN} \cdot R3}$$

Additional diode/resistor combinations can be added to further contour the gain.

FIGURE 27: Current Monitor Circuit

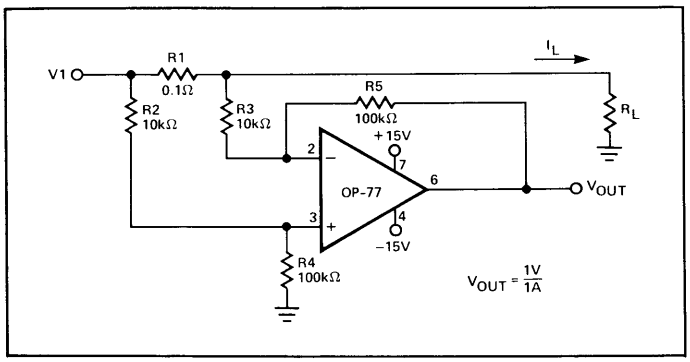

This versatile monitor circuit can typically sense current at any point between the ±15V supplies ($|V1| < 14.3V$ guaranteed). This makes it ideal for sensing current in applications such as full bridge drivers where bi-directional current is associated with large common-mode voltage changes. The 120db CMRR of the OP-77 makes the amplifier's contribution to common-mode error negligible, leaving only the error due to the resistor ratio inequality. Ideally, R2/R4 = R3/R5. This is best trimmed via R4.

FIGURE 28: Free-Running Square-Wave Oscillator

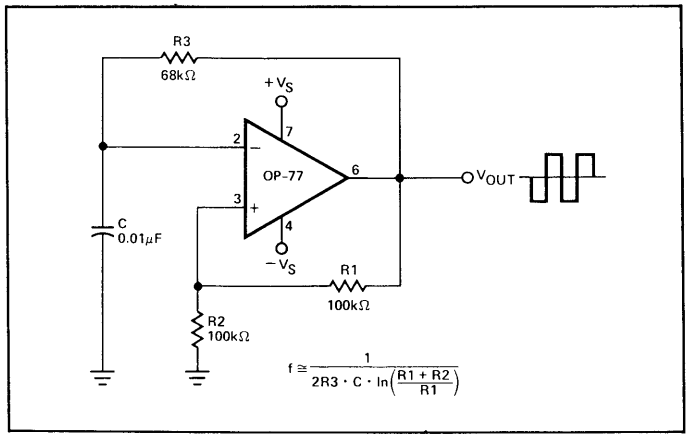

This simple oscillator creates a square-wave output of $\pm(V_S - 2V)$ at 1kHz for the values shown.

FIGURE 29: Precision Analog Multiplier/Divider

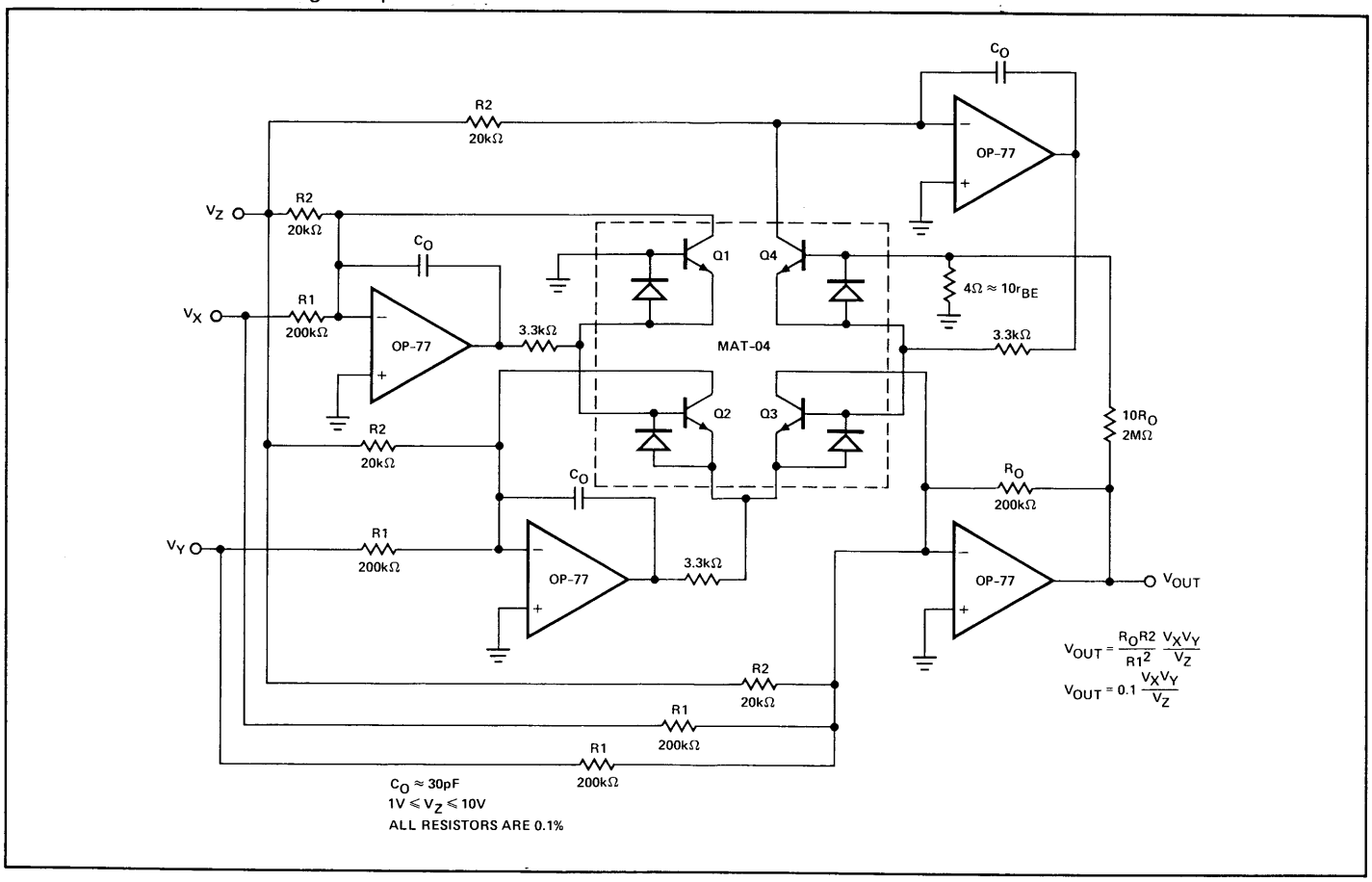

This multiplier/divider achieves its excellent performance through the low emitter resistance, r_{BE}, and superior V_{OS} matching of MAT-04 quad transistor array. In this circuit, linearity error due the transistors is less than ±0.1%. The OP-77 helps maintain accuracy with a V_{OS} less than 25μV. For even higher accuracy the offset voltages may be nulled.

FIGURE 30: Precision Absolute Value Amplifier

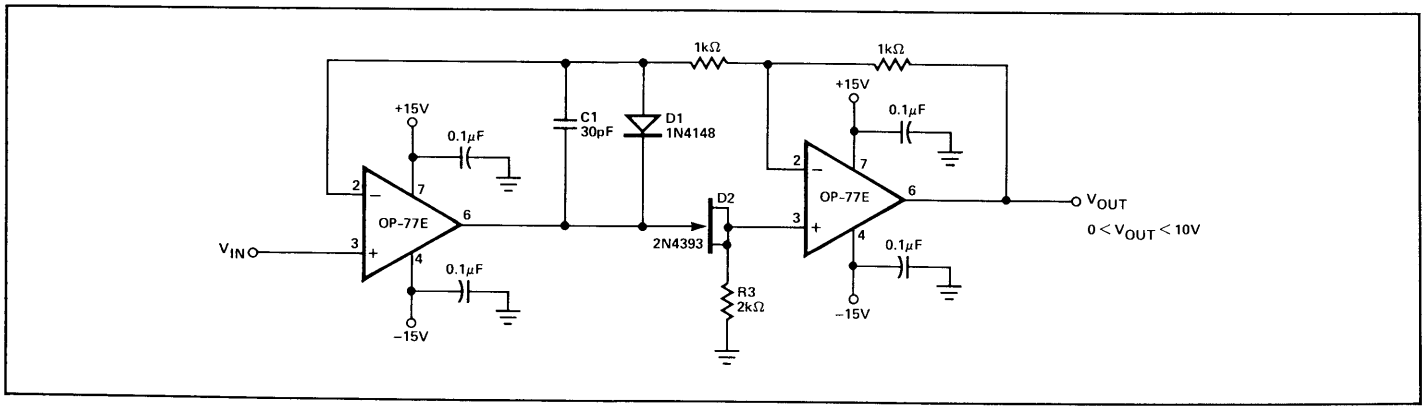

The high gain and low TCV_{OS} assure accurate operation with inputs from microvolts to volts. In this circuit, the signal always appears as a common-mode signal to the op amps. The OP-77E CMRR of 1μV/V assures errors of less than 2ppm.

FIGURE 31: Thermocouple Amplifier With Cold-Junction Compensation

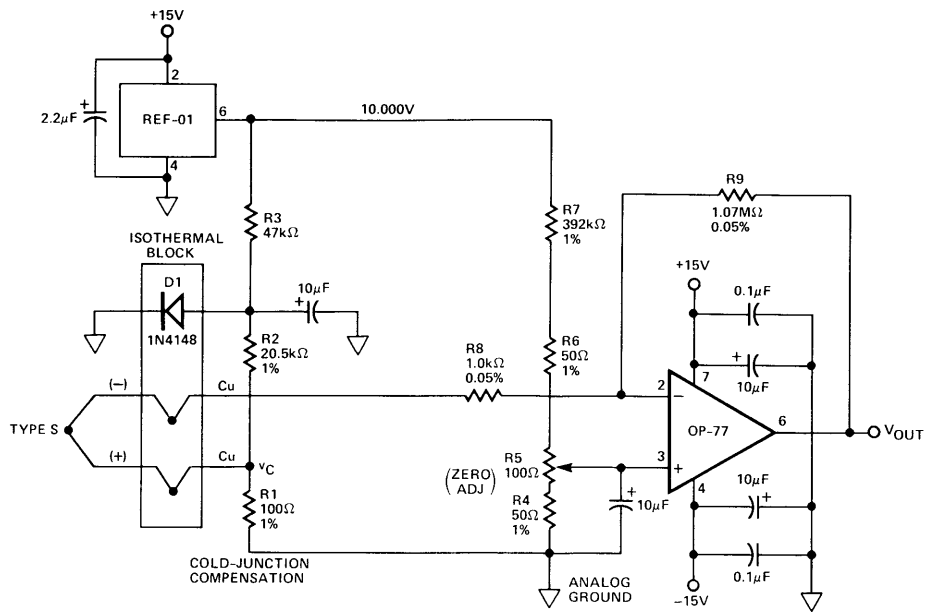

The high gain, low noise, and low offset drift of the OP-77 can be used to create a thermocouple amplifier with superb linearity. They combine to give a total accuracy typically better than ±0.5°C.

Cold-junction compensation is performed by R1, R2, and D1 which is mounted isothermally with the thermocouple terminating junctions. Calibration is done using R5 after the circuit has stabilized for about 15 minutes. A copper wire short is applied across the terminating junctions simulating a zero °C ice point. R5 is then adjusted for 0.000V output. The short is then removed, and the amplifier is ready for use.

This amplifier can be used for type S, J, and K thermocouples with the appropriate resistor values as shown below. R9 is chosen to give a +10.000V output for a 1,000°C measurement.

TYPE	SEEBECK COEFFICIENT, α	R1	R2	R7	R9
K	39.2µV/°C	110Ω	5.76kΩ	102kΩ	269kΩ
J	50.2µV/°C	100Ω	4.02kΩ	80.6kΩ	200kΩ
S	10.3µV/°C	100Ω	20.5kΩ	392kΩ	1.07MΩ

FIGURE 32: Instrumentation Amplifier (2 Op Amp Design)

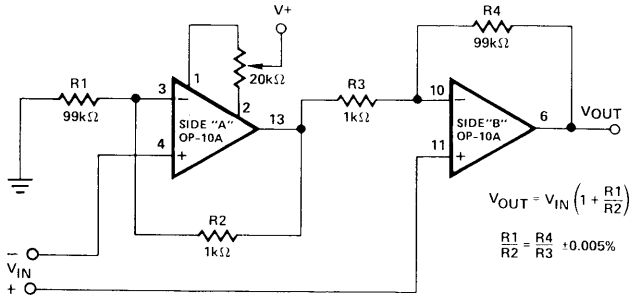

This differential amplifier offers high input impedance and a power supply rejection ratio greater than 100dB. Because the high circuit gain occurs in Side "B"; Side "A" offset should be adjusted with respect to V_{OUT}. This simultaneously corrects for Side "B" offset voltage. For the circuit values given, $A_V = 100$.

FIGURE 33: ±200V Low Offset Operational Amplifier

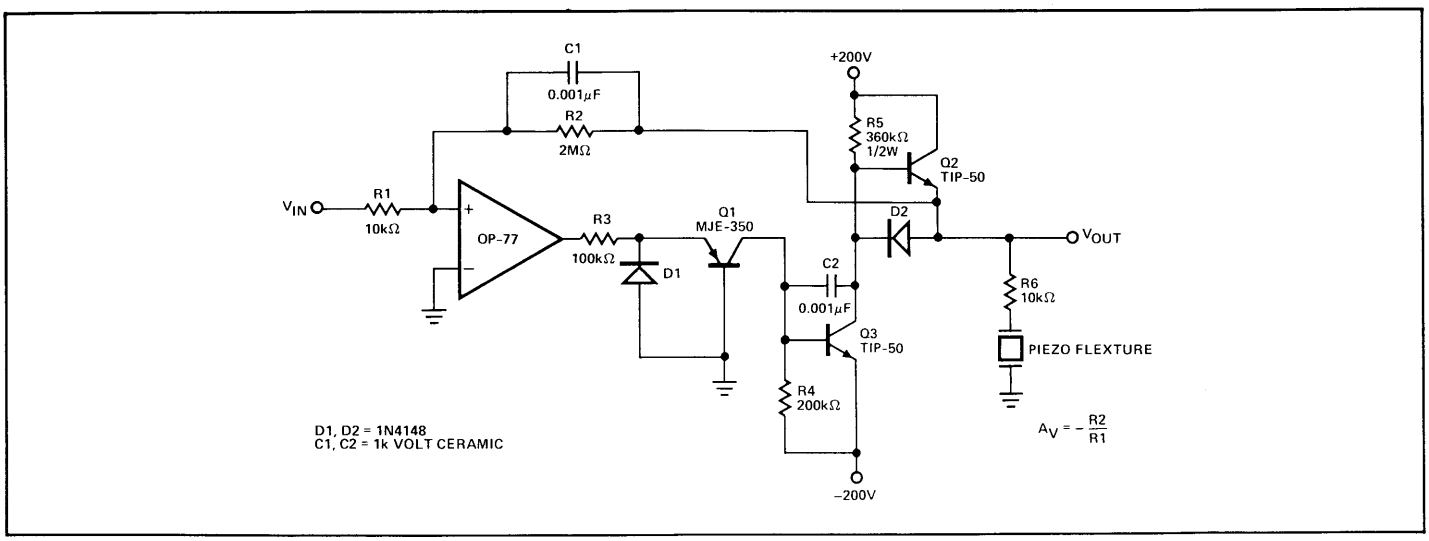

The OP-77 is the heart of this high voltage amplifier designed to drive piezo flexture elements in precise positioning applications. The high gain and low offset voltage of the OP-77 produce an accurate, stable drive voltage to the piezo device allowing predictable, repeatable sub-micron movements to be easily controlled.

The output of the OP-77 creates a proportional current drive through the common-base connected Q1 to the base of Q3. Q3 forms a Class A amplifier with bias resistor R5, and transistor Q2 is simply an emitter-follower used for output current boost. R6 is necessary to prevent oscillation caused by the capacitive loading of the piezo device on the output of the amplifier.

FIGURE 34: Impedance Transforming Amplifier

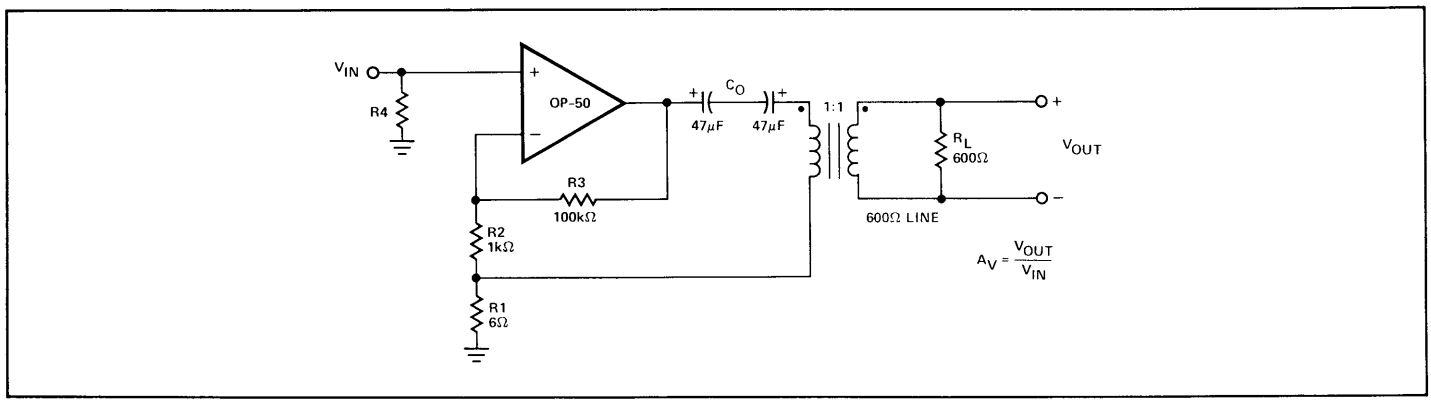

This is an efficient, flexible circuit simulating a source impedance equal to the load impedance. By definition, if $R_S = R_L$, then,

$$A_V = \frac{A_{V(UNLOADED)}}{2}$$

The unloaded gain is roughly R3/R2. When the output is loaded, a second feedback loop is closed whose gain, $A_V \simeq R_L/R1$, combines in parallel with $A_{V(UNLOADED)}$ to give:

$$A_{V(LOADED)} = \frac{A_{V(UNLOADED)} \cdot A_V}{A_{V(UNLOADED)} + A_V}$$

If $R3/R2 = R_L/R1$, then $A_{V(LOADED)} = \frac{A_{V(UNLOADED)}}{2}$

These approximations assume that $R1 \ll R2$ and $R2 \ll R3$. The OP-50 requires no compensation for the circuit values shown and can easily drive the 600Ω line.

FIGURE 35: Precision Current Sinks

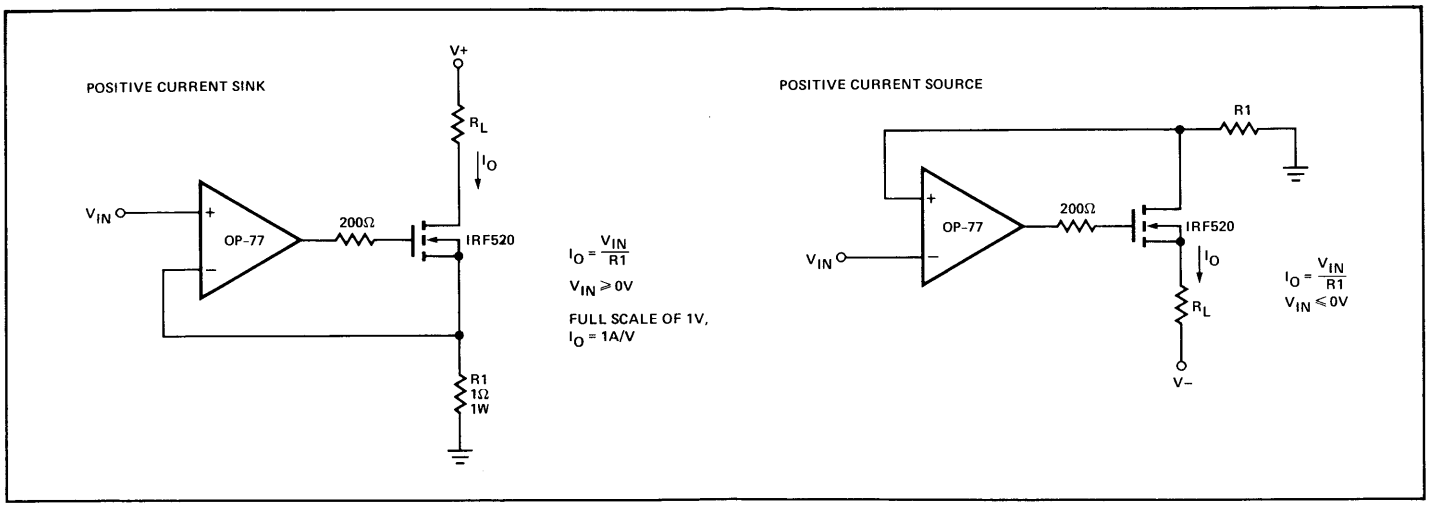

These simple high-current sinks require that the load float between the power supply and the sink. In these circuits, OP-77's high gain, high CMRR, and low TCV_{OS} assure high accuracy.

FIGURE 36: Low Noise AGC Amplifier

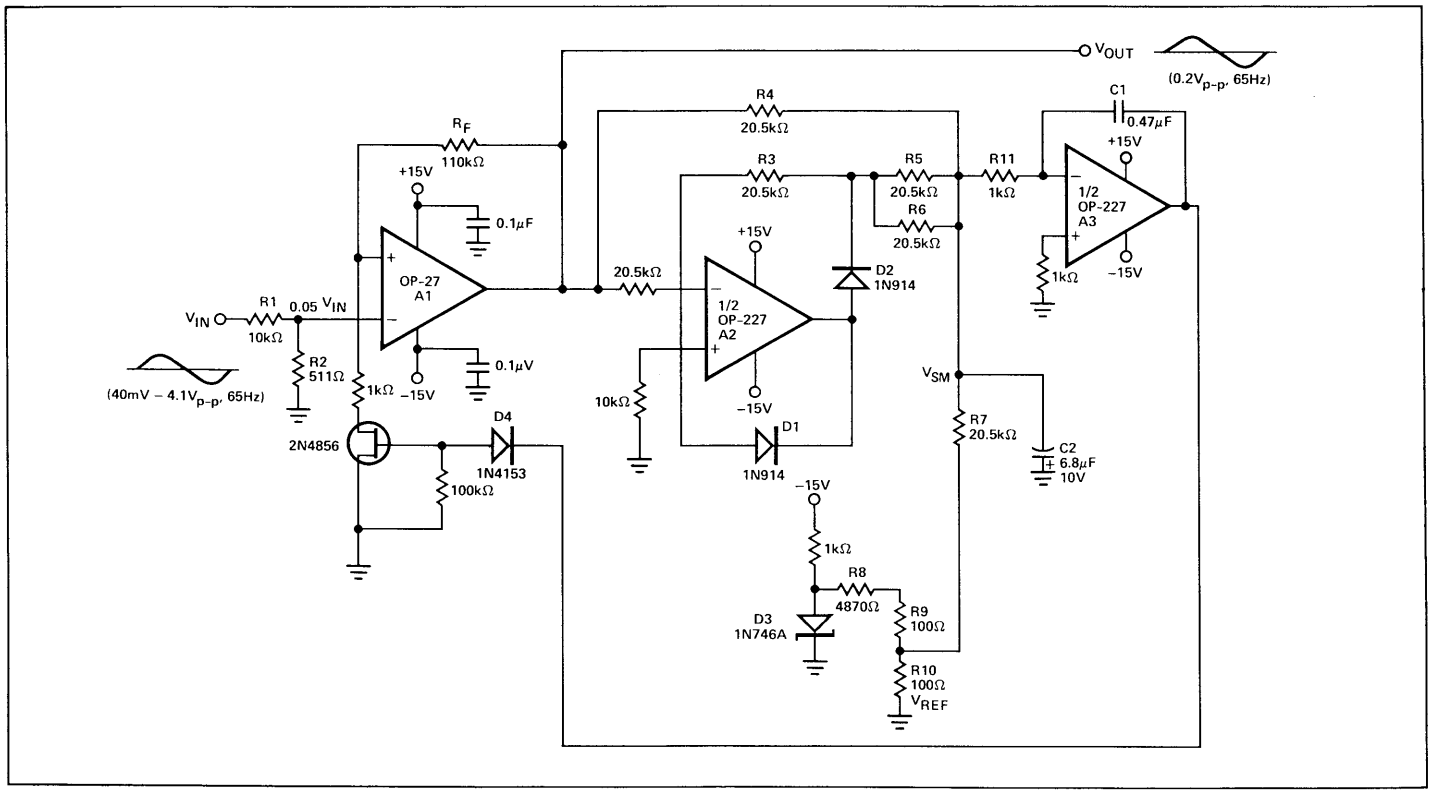

In this circuit, a JFET transistor is used to control the gain of the low-noise OP-27 amplifier over a two-decade input voltage range. For inputs from 40mV to 4.1V peak-to-peak, the AGC maintains a 0.2V peak-to-peak output.

Amplifier A2 performs an absolute-value operation on V_{OUT} and sums the result with a –0.2V reference on capaciator C2. The deviation of this sum, V_{SM}, from zero is amplified by A3 and controls the gate of the JFET. If the peak-to-peak amplitude of V_{OUT} exceeds 0.2V, V_{SM} becomes positive and drives the JFET gate negative. This increases the JFET's channel resistance lowering the gain of the A1. The reverse of this occurs if V_{OUT} falls below 0.2V peak-to-peak.

The values of C1 and C2 are chosen to optimize the circuits response time for a given input voltage frequency. This example was designed for a 65Hz signal. Higher frequencies would justify lower values for C1 and C2 to speed the AGC response.

FIGURE 37: Amplifier with Active Output Clipping

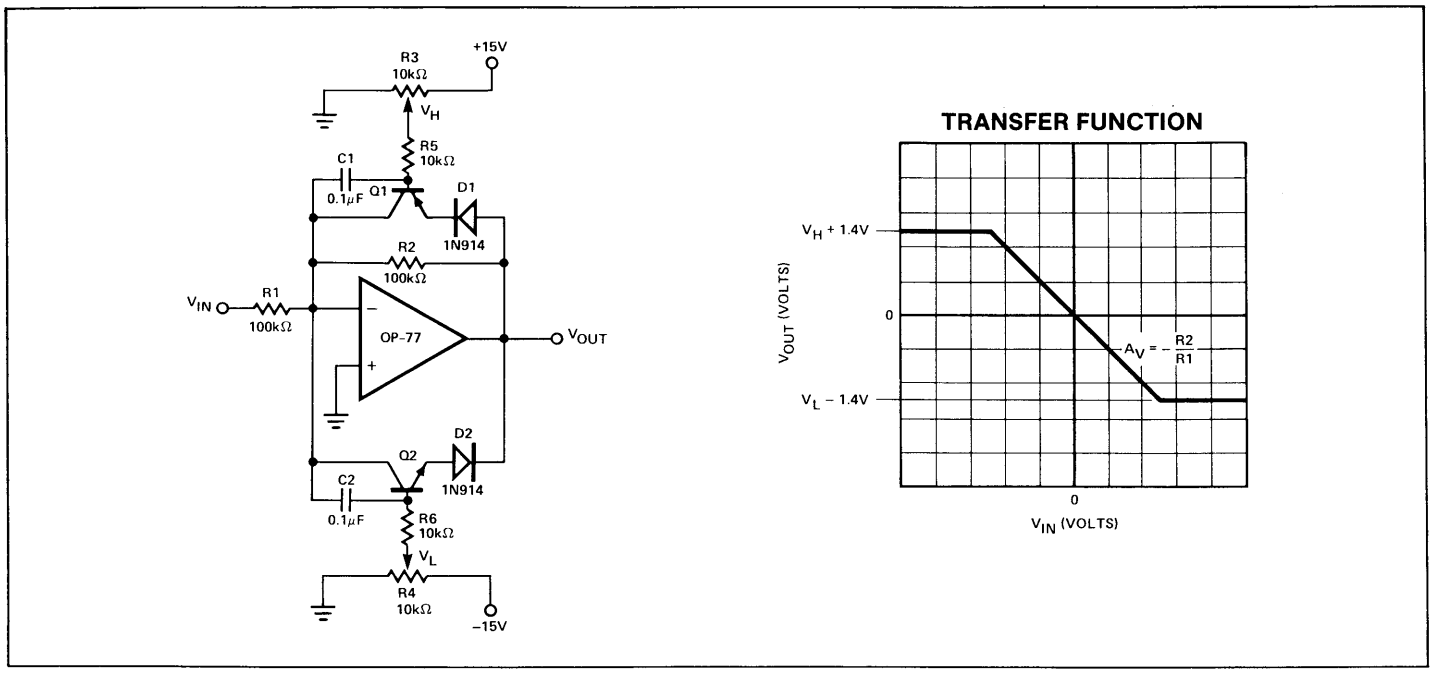

This configuration allows adjustment of the op amp's maximum output voltage. Below the clipping levels, circuit gain is $A_V = -R2/R1$. As V_{OUT} rises above ($V_H + 1.4V$), the base/emitter of Q1 becomes forward biased, allowing collector current to flow to the summing node, thus clamping V_{OUT}. A similar action occurs as V_{OUT} goes below ($V_L - 1.4V$) and is clamped by Q2.

FIGURE 38: Low Power Amplifier With Squelch

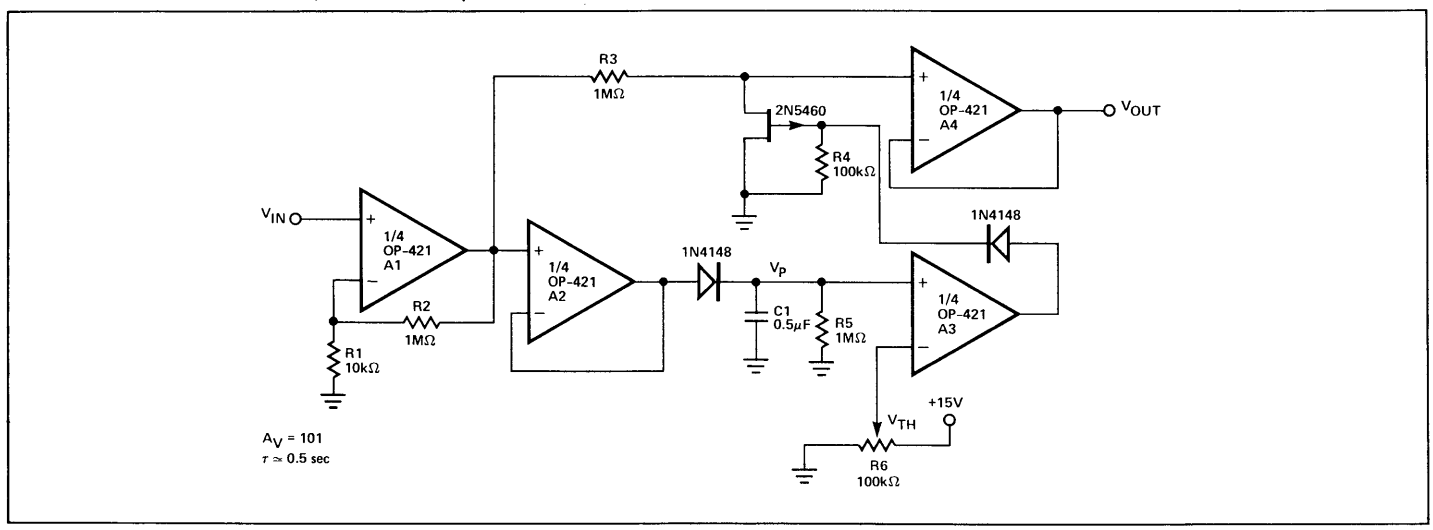

The OP-421 is the heart of this variable squelch amplifier which requires less than 2mA of supply current ($R_L = \infty$). A1 provides a high impedance input amplifier with $A_V = 1 + R2/R1$. Its output drives a unity gain output buffer, A4, and a peak detector with a time constant set by C1 and R5. When the output of the peak detector, V_P, exceeds the adjustable threshold, V_{TH}, the comparator, A3, drives the gate of the P-channel FET high, turning it OFF. At lower input signal levels, V_P falls below V_{TH}, and the FET turns ON, clamping the input of A4 to ground.